

Scalable Many-Objective Pathfinding Benchmark Suite

Jens Weise, *Member, IEEE*, and Sanaz Mostaghim, *Senior Member, IEEE*

Abstract—THIS IS A PREPRINT SUBMITTED TO arxiv.org. IT CAN BE SUBSTITUTED WITH A NEWER VERSION AT ANY TIME.

Route planning also known as pathfinding is one of the key elements in logistics, mobile robotics and other applications, where engineers face many conflicting objectives. However, most of the current route planning algorithms consider only up to three objectives. In this paper, we propose a scalable many-objective benchmark problem covering most of the important features for routing applications based on real-world data. We define five objective functions representing distance, traveling time, delays caused by accidents, and two route specific features such as curvature and elevation. We analyse several different instances for this test problem and provide their true Pareto-front to analyse the problem difficulties. We apply three well-known evolutionary multi-objective algorithms. Since this test benchmark can be easily transferred to real-world routing problems, we construct a routing problem from OpenStreetMap data. We evaluate the three optimisation algorithms and observe that we are able to provide promising results for such a real-world application. The proposed benchmark represents a scalable many-objective route planning optimisation problem enabling researchers and engineers to evaluate their many-objective approaches.

Index Terms—route finding, benchmark, many-objective optimisation, evolutionary algorithm

I. INTRODUCTION

Optimal route planning (or pathfinding) is among the most challenging tasks for industrial and logistical applications [1]. Any improvement in the results can have a considerable impact on many factors, such as fuel consumption and the environment. The current state-of-the-art route planning algorithms usually consider the travel time and the distance in the optimisation. However, specific applications encounter additional criteria such as the curvature of the route, the elevation (ascent), or environmental issues such as air pollution caused by fuel consumption. These criteria can profoundly influence the practicability of the solutions. For instance, for animal transportation, we need to additionally minimise the number of curves in the route (or maximise the smoothness). Reducing the length of the route can help to reduce fuel consumption, while possibly increasing the travelling time. Other criteria such as the ascent of a path can be considered for heavy vehicles which can consume more fuel on such non-flat routes.

The goal of this paper is to propose a many-objective route planning problem representing five objective functions which at the same time are highly related to their real-world

counterparts. This real-world problem can be considered as scalable in terms of complexity, since the size of the search space can be varied, influencing the objective functions as well in terms of search space size. To the best of our knowledge, there is no work in the literature which considers all of these criteria at the same time. Similar to the existing navigation and route planning algorithms, we work on a graph-based approach for addressing this many-objective problem. We additionally apply the benchmark characteristics to the real-world data from OpenStreetMap in Berlin.

Our results show that this problem can be used both as a benchmark and as well as a real-world application. We additionally provide the true Pareto-front of 491 benchmark instances, their respective Pareto-sets and the code to generate specific instances of the proposed benchmark.

The paper is structured as follows. In Section II, we provide an overview of the related works. Section III is dedicated to the many-objective pathfinding problem, the proposed encoding and the objective functions. In section V, we provide experiments using three state-of-the-art optimisation algorithms, and in Section V-D, we transfer the benchmark and objective functions to real-world road map data. Section VI concludes the paper and gives an overview of future work.

II. RELATED WORKS

There is an extensive amount of literature in the field of route planning and pathfinding in general and especially for vehicle route planning which uses evolutionary algorithms [2], [3], [4], [5]. The most important feature concerns the solution representation, which can define the size of the search space and influence the efficiency of the algorithms.

Various representations such as graph-based [6], [7], [8], [9], [10], [11], and grid-based representations [2], [12] have been suggested for the pathfinding problem. Typically, there are two main approaches: The first is a variable-length chromosome representation which is often used in combination with the graph-based problem representation [13], [14], [15], [16]. This approach represents a solution as a list of nodes, which can be of different length when computing a path. The second approach is a fixed-length chromosome, representing the directions of travel together with a list of nodes in a graph or a list of grid cells [17], [18], [2]. Grid-based representations for pathfinding problems are shown to be very practical for evolutionary algorithms [2], [5]. Such grid representations can be refined depending on the required resolution of the problem. Moreover, they are often used for benchmarking purposes [19], [20]. Also, they can represent the real-world problems abstractly by discretising the problem representation [21]. Grids

J. Weise and S. Mostaghim are with the Institute for Intelligent Cooperating Systems, Otto von Guericke University Magdeburg, Germany e-mail: {jens.weise,sanaz.mostaghim}@ovgu.de.

typically consist of units with adjustable sizes [22]. An encoding can consist of a linked-list of units [23], the directions [2], or the coordinates of several waypoints.

It is comparatively easy to convert a grid into a graph by considering units as nodes and their contact-edges as the graph's edges. This is done in several applications, e.g. the game industry when it comes to pathfinding, by superimposing a grid over an area and using graph-search algorithms [24]. The commonly used A* algorithm is an example of pathfinding on a grid which is transferred to a graph [24], [19].

In general, graph-based representations allow a higher flexibility in representing real-world problems, which can be considered heterogeneous, compared to grids which are usually homogeneous. Due to this, in this paper, we present the proposed benchmark problem as a grid transferred to a graph and facilitate the methods to evaluate them on realistic graph-represented road map data.

Route planning techniques can be applied to applications as pipe- or wire-routing [25]. Weise et al. used a customised NSGA-II algorithm for a multi-objective generation of wiring harnesses [26] and optimised length and the maximum heat for a wire which is confronted in a path. Oleiwi et al. used a hybrid approach by modifying a genetic algorithm based on the A* algorithm [27]. Changan and Quiongbing used genetic algorithms and customised operators to work on the pathfinding problem [6], [7].

Considering many-objective pathfinding problems, there is a limited amount of literature using evolutionary algorithms. Tozer et al. [8] provide an overview of existing approaches and use reinforcement learning to address the problem with six objective functions. Pulido et al. [9] introduce a dimensionality reduction technique in order to minimise dominance checks during the optimisation and tested their algorithm on a map from a real-world application. They extended the NAMOA* algorithm, which was first introduced by Mandow [28] and is a multi-objective extension to the well-known A* algorithm [29]. Considering many-objective benchmarks in general, there are several existing benchmark frameworks and functions available [30], [31].

III. MANY-OBJECTIVE PATHFINDING PROBLEM

In this section, we propose a many-objective pathfinding problem which can be additionally used as a benchmark problem with a scalable size of the search space. As the benchmark aims to represent environments for pathfinding algorithms for maps, we construct the instances by defining a cartesian grid with a specific size, where each cell has the same dimensions, also known as *integer lattice*. The variable properties of the benchmark influence the properties of each cell in the lattice.

A. Benchmark problem construction

The multi-objective route planning problem, hereafter called *pathfinding problem*, can be defined as a network-flow problem [32], [9]. The goal is to find a set of optimal paths (routes) $P^* = \{p_1, \dots, p_L\}$ in a graph $G(V, E)$ from a starting node $n_S \in V$ to a pre-defined end node $n_{End} \in V$, i.e.,

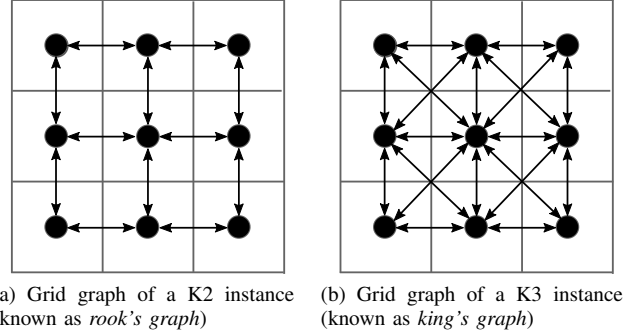
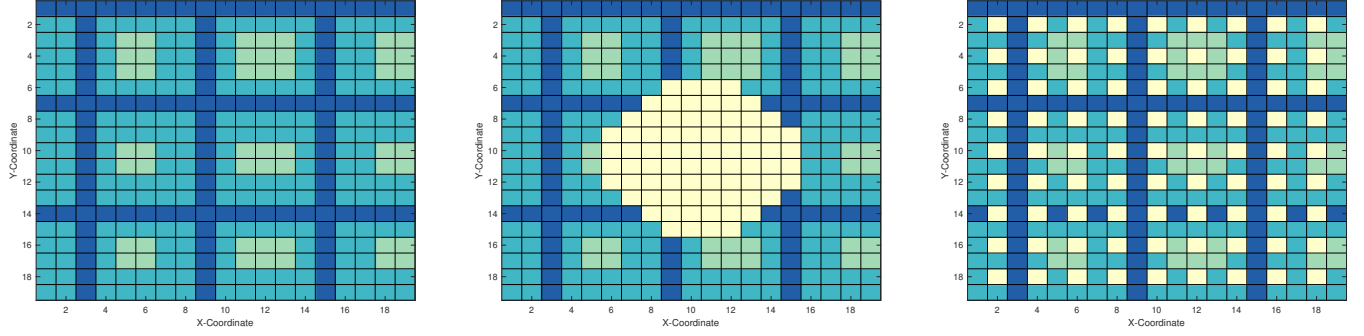


Fig. 1. Superimposed graphs on their respective grids

$p_i = (n_S, \dots, n_{End})$ for path N_i . Before constructing the problem-related graph, we model a grid which is used as a map for the pathfinding problem. We assume to have a two-dimensional search space defined by a given size (i.e. size of the map) denoted by the range $[x_{min}, y_{min}]$ and $[x_{max}, y_{max}]$, $x, y \in \mathbb{N}$. This search space is divided into grid cells which define the resolution of the path planning and therefore, the size of the search space. We define different types of grid cells which impose constraints on the velocity of movements indicated by v_{max} representing different road types as well as obstacles where a movement cannot occur.

We furthermore define an elevation function h with a variable number of hills which can be defined by either using a peak-function or a combination of hill functions. Two more features concern the neighborhood and backtracking. The neighbourhood property defines the possible neighbour cells to which an agent can move. We use the 2^k -neighbourhood similar to [33]. In this case, $k = 2$ means that it is possible to go to one of the four neighbours, located in the cardinal directions, where $k = 3$ defines eight possible neighbours, taking the diagonal cells into account. The backtracking property of the benchmark defines if an agent can go backwards or only forward. For instance, if backtracking is allowed and the goal is to go from the north-west corner of the grid to the southern-east one, the agent can go in any direction specified by the 2^k -neighbourhood from any cell on a certain path. If backtracking is not allowed, the agent can only move in the directions of east, south and south-east (if $k = 3$). An 8-neighbourhood with enabled backtracking is also known as *king-moves*, derived from chess.

In the following, we propose a graph-based representation of the benchmark grid. Therefore, we describe all objectives for the evaluation of a *solution* represented as a path N of length K consisting of a list of adjacent nodes in a graph $G = (V, E)$: $N = (n_i, n_{i+1}, \dots, n_k)$. However, for the evaluation on the grid (as described above), the nodes n_i can be replaced by their respective coordinates (x_i, y_i) . Each cell i of the grid is represented as a node n_i located on the coordinate (x_i, y_i) , and depending on the 2^k -neighbourhood and backtracking property, the corresponding neighbours are connected using edges. The resulting graph is also known as *grid graph* or *lattice graph*. Figure 1 visually shows an example of the transfer from a grid to a graph.



(a) three different types of cells ($v_{max}(blue) > v_{max}(turquoise) > v_{max}(brightyellow) > 0$). (b) lake-obstacle with $v_{max} = 0$ in the middle of the map. (c) checkboard-obstacles representing a block-like infrastructure

Fig. 2. Different grid cell properties

B. Objective functions

Given a solution represented by a path N of length K as $N = (n_i, n_{i+1}, \dots, n_k)$, we can evaluate it by five objectives to be minimised: (1) Euclidean length, (2) Delays, (3) Elevation, (4) Traveling time and (5) Smoothness (Curvature).

Objective 1: Euclidean length

The Euclidean length represents the distance between the start n_S and the end n_{End} of a path. It is calculated by the sum of the Euclidean distances $d(n_{i-1}, n_i)$ between the neighbouring vertex pairs n_{i-1} and n_i in a solution path N as follows:

$$f_1(N) = \sum_{i=1}^{K-1} d(n_i, n_{i+1}) \quad (1)$$

$$d(u, v) = \|u - v\|_2 \quad (2)$$

We consider that $i = 1$ corresponds to the starting point n_S and the last node of a path n_K maps to the endpoint denoted n_{End} . Figure 3 illustrates an example. In real-world applications, this objective can be additionally used to estimate fuel consumption.

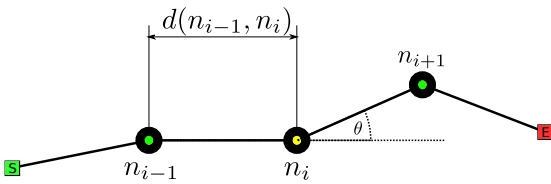


Fig. 3. Objectives (1) and (5) on an example path, which is modeled using a graph with nodes and edges.

Objective 2: Delays

The second objective is meant to measure the amount of delay in a given path. In real-world applications, delays are caused by accidents or traffic. Therefore, a delay is the likelihood of having an accident on each node of the path. The delay per path segment between the nodes n_i and n_{i+1} is defined by the differences between the corresponding values of the two adjacent nodes. Our proposed second objective f_2 calculates the sum of *delay* for all the edges on a given path N :

$$f_2(N) = \sum_{i=1}^{K-1} delay(n_i, n_{i+1}) \quad (3a)$$

$$delay(n_i, n_{i+1}) =$$

$$\begin{cases} 2 & \text{if } v(n) \neq v(n_1) \\ 3 & \text{if } v(n) = \text{city} \wedge v(n_1) = \text{city} \\ 1 & \text{if } v(n) = \text{country} \wedge v(n_1) = \text{country} \\ \frac{1}{5} & \text{otherwise} \end{cases} \quad (3b)$$

Objective 3: Elevation

The aggregated ascent of a solution path is represented in the third objective. Similar to the second objective, this objective is also defined on a grid map. Our proposed benchmark contains various possibilities for defining the elevation function $h(n_i)$ which is defined on a node n_i . Examples of the elevation function are shown in fig. 4. The ascent is calculated between two nodes in the graph $e(n_i, n_{i+1})$. and the third objective $f_3(N)$ is the sum of the elevations between all the nodes in a path N :

$$f_3(N) = \sum_{i=1}^{K-1} e(n_i, n_{i+1}) \quad (4)$$

$$e(m, n) = \begin{cases} h(m) - h(n), & \text{if } h(m) > h(n) \\ 0, & \text{else} \end{cases}$$

Similar to objective 1, this objective also represents the amount of fuel consumption. Figure 4 shows an example of the elevation function.

Objective 4: Traveling time

The fourth objective represents the traveling time. For this purpose, we utilize the velocity defined by $v_{max}(n_i)$ for each node n_i and use the length of the path which was also used for the Objective 1:

$$f_4(N) = \sum_{i=1}^{K-1} \frac{2d(n_i, n_{i+1})}{v_{max}(n_i) + v_{max}(n_{i+1})} \quad (5)$$

Objective 5: Smoothness

The smoothness, or curvature, of a path is modeled in the fifth objective. We measure smoothness by calculating the angle between three nodes on a path, as shown in Figure 3. The angle θ is obtained by extending the line between two nodes and measuring the angle to the third node. Similar to [27], [14], we invert $a \cdot b = \|a\| \|b\| \cos(\theta)$:

$$f_5(N) = \sum_{i=2}^{K-1} \arccos\left(\frac{\vec{n_i n_{i-1}} \cdot \vec{n_{i+1} n_i}}{|\vec{n_i n_{i-1}}| \cdot |\vec{n_{i+1} n_i}|}\right) \quad (6)$$

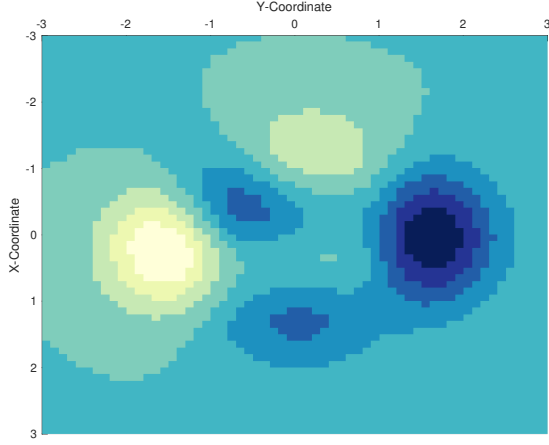


Fig. 4. Example of elevation function h illustrated by contours. Dark colors illustrate the amount of elevation

Since we intend to minimise the objective values, the smaller smoothness value represents a more straight path.

IV. BENCHMARK TEST SUITE

Given the above model, we can generate several problem instances. In the following, we propose various examples for a test suite by selecting specific features for the defined variables of the benchmark. We set 4 various kinds of cells with velocity values $v_{max}(Highway) = 130 \frac{km}{h}$, $v_{max}(Country) = 100 \frac{km}{h}$ and $v_{max}(City) = 50 \frac{km}{h}$. As for obstacle cells ($v_{max} = 0$), we propose two different forms: 1) the checkerboard pattern is designed to simulate block-like environments, and 2) the lake obstacle denotes a large region which is not passable. For the checkerboard obstacles, every second cell is defined as an obstacle in both x and y directions. The lake obstacle is defined as a circle on the grid. The circle radius is defined by a fraction of the x -size of the square wave function and circle function, respectively. Equations (8a) and (9a) describe the obstacle as a variant of the square wave function and circle function, respectively. In the tested instances, the Lake obstacles are defined by a radius of $0.25x_{max}$. Figures 2b to 2c shows the two obstacle types on an example instance of the benchmark problem. Figure 2a shows an example instance of size 20. The darkest grid cells represent large speed grids (motorways), the lighter colored cells represent paths with smaller velocity values and the lightest colors indicate the obstacles with $v_{max} = 0$.

$$v_{max}(x, y) = \begin{cases} v_H, & \text{if } w(x, y) > 0.9 \\ v_S, & \text{if } w(x, y) < -0.4 \\ v_M, & \text{else} \end{cases} \quad (7)$$

$$w(x, y) = \max(\sin(x), \cos(y))$$

$$g_{CH}(x, y) = \text{sign}\left(\sin\left(\frac{\pi}{2} + \pi x\right)\right) + \text{sign}\left(\sin\left(\frac{\pi}{2} + \pi y\right)\right) - 2 \Pi(x - x_{max}) \Pi(y - y_{max}) < 2 \quad (8a)$$

$$\Pi(x) = H\left(x + \frac{1}{2}\right) - H\left(x - \frac{1}{2}\right) \quad (8b)$$

where $H(x)$ is the Heaviside step function

$$g_{LA}(x, y) = \left(x - \frac{x_{max}}{2}\right)^2 + \left(y - \frac{y_{max}}{2}\right)^2 - (r x_{max})^2 < 0$$

where r denotes the radius ratio

(9a)

As for the elevation, we set four hill functions in the domain $(-3, 3)$ which will be scaled when applied to the grid with cell coordinates (x, y) represented by the node n in the path segment:

$$h_1(x, y) = 3(1-x)^2 e^{-x^2 - (y+1)^2} - 10e^{-x^2 - y^2} (-x^3 + x/5 - y^5) - 1/3 e^{-(x+1)^2 - y^2}$$

$$h_2(x, y) = 5e^{-(x+1.5)^2 - (y+1.5)^2} \quad (10)$$

$$h_3(x, y) = 5e^{-(x-1.5)^2 - (y-1.5)^2}$$

$$h_4(x, y) = 5e^{-(x-1.5)^2 - (y+1.5)^2}$$

These functions can be linearly combined which can produce many variations for the elevation function h :

$$h(x, y) = \sum_{i=1}^{nh} h_i, \quad nh = \{1, 2, 3, 4\} \quad (11)$$

For the third objective, we aggregate positive slopes, as we want to focus on flat routes. Taking also negative elevations into account could result in a path containing a hill with a high steep which would not be beneficial to bulky goods transports.

All these variations of the properties are used in the name of a benchmark instance. The name starts with *ASLETISMAC* for the five objectives to be minimised (Ascent, Length, Time, Smoothness and Accidents), then the obstacle type, followed by the size in X and Y directions, then the elevation function is represented (PM stands for the peaks-function h_1 and the combination is set to Pnh), followed by the 2^k -neighbourhood and the backtracking property (B followed by T for True or F for False). For example, *ASLETISMAC_CH_X10_Y10_P1_K2_BF* defines an instance with the checkerboard obstacles, sized 10×10 , $nh = 1$ as the elevation function, four possible neighbours ($K2 \rightarrow 2^2 = 4$), but no backtracking (BF).

For the values of delays in the second objective, we can refer to real-world statistical data (see eq. (3a))¹.

A. Obtaining the true Pareto-Front

In order to make this benchmark-framework available, we performed an exhaustive search on 289 benchmark instances with different obstacle types, sizes, elevation-functions, neighbourhood metrics but only without backtracking, since these instances were too complex to provide any meaningful algorithmic results. However, the benchmark contains these as well, and we want to investigate these instances in the future as well. We provide the corresponding 273 Pareto-Fronts and their corresponding sets for the five-objective optimisation. The missing 16 instances do not have any solution due to the nature of the benchmark, i.e. the lake

¹https://www.destatis.de/EN/Themes/Society-Environment/Traffic-Accidents/_node.html

obstacle covers too much of the area. Depending on the type, there are different numbers of Pareto-optimal solutions. In order to obtain the fronts, we performed a depth-first search (DFS) from the cell at the northern-west corner to the south-east corner cell. The larger the instances are, the longer the DFS takes to complete. The most complex in terms of the number of possible paths, which we evaluated, is the instance *ASLETISMAC_NO_X14_Y14_PX_K3_BF*, that has a size of 14x14, 4-neighbourhood and no backtracking. For this instance, there are 1,409,933,619 possible paths.

We implemented an exhaustive search by running the DFS as mentioned earlier and evaluated the solutions according to the objectives specified in section III-B for all the 289 instances. After the evaluations, we calculated the non-dominated set representing the true Pareto-front (provided together with the codes in supplementary materials).

V. EXPERIMENTS

In the experiments, we aim to investigate the many-objective pathfinding problem for one instance of the benchmark and provide an in-depth analysis of the proposed objective functions. We perform three different state-of-the-art evolutionary algorithms on several instances to evaluate the complexity of the benchmark. Furthermore, we present a custom mutation operator, which can operate on a variable-length chromosome consisting of a list of nodes.

A. Search space encoding and operators

In our proposed benchmark, we consider a solution to be a sequence of nodes $N = (n_1, \dots, n_K)$ with a variable-length K . We take this representation for the encoding in evolutionary algorithms. The variable-length chromosome poses difficulties for the algorithms but can be very efficient when using realistic data since intersections and endpoints are not homogeneously distributed, and paths usually have different lengths. This representation has been used by [34], [35], [36] and studied by [37].

We use a one- or two-point cross-over for this encoding as follows. If two selected solutions have intersection points except for the start and end nodes, these points can be used as possible cut-off points. If there are fewer than two intersections, we use a one-point cross-over. Additionally, we define the so-called *perimeter mutation operator*. From a given path which is to be mutated, we took two arbitrary points within a maximum network distance $d_{max} = \frac{|N|}{2}$ and compute their middle point. We then search for a random point in the network within a maximum distance of r_{max} , using an R-Tree index from that point. Then we perform a random-search (local search) from the first and second points to it. Depending on the benchmark instance, we either consider all neighboring nodes within the radius in positive cardinal and diagonal directions (instances of type *K3,BF*) or a subset of them: nodes in positive cardinal directions for *K2,BF*.

B. Experiment setup

In the experiments, we use the NSGA-II [38], NSGA-III [39] and DIR-enhanced NSGA-II (d-NSGA-II) [40] algorithms. The d-NSGA-II uses a diversity indicator based on

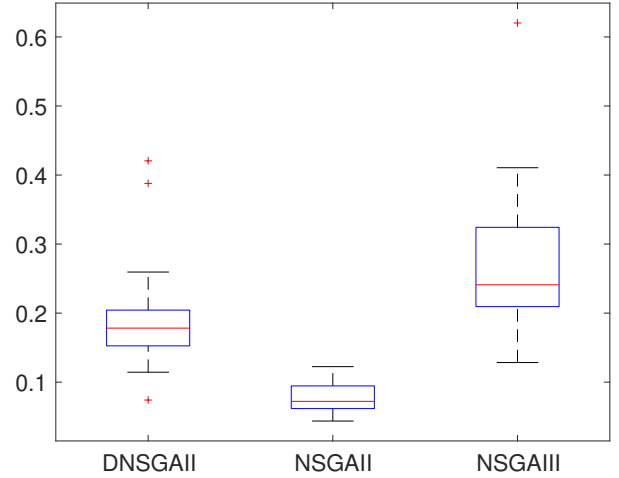


Fig. 5. Obtained IGD⁺ Values for the instance ASLETISMAC_NO_X14_Y14_PM_K3_BF

reference vectors [40], making it suitable for many-objective optimisation problems. For all three algorithms, we set the population size to 212 as in the original NSGA-III study. We set the probabilities for cross-over and mutation to 0.8 and 0.2, the number of divisions for NSGA-III to $p = 6$, maximum number of generations to 500, and all for 31 runs for statistical analysis. The task of the pathfinding algorithm is to find a path from the north-west corner to the south-east corner. We take 273 problem instances:

We implemented the experiments using the JGraphT library [41] for graph storage and the jMetal framework, version 6.0 (development snapshot), for the algorithm's execution [42]. To compare the algorithms, we calculated the IGD⁺ indicator [43], [44]. The results are compared and tested for statistical significance using the two-sided pairwise Mann-Whitney-U Test, with the null hypothesis that the distributions of the three samples have equal medians. Statistical significance of the differences between the performance is assumed for a p-value smaller than 0.01.

C. Results

In the first part of our analysis, we count the number of successful runs in which the algorithms could obtain the entire Pareto-front. A front is found if the IGD⁺ is 0 in all 31 runs on the algorithms. Given 273 valid instances, NSGA-II, NSGA-III and d-NSGA-II were not able to find the front for 235, 234 and 241 instances. This indicates the difficulty of the benchmark for certain instances. Figure 5 shows the obtained IGD⁺ values for the instance *ASLETISMAC_NO_X14_Y14_PM_K3_BF* for which none of the algorithms found the whole Pareto-front, indicating complexity of the problem. We observe that NSGA-II obtains the best result, even if NSGA-II is not the best option for many-objective problems.

Overall, NSGA-II performed the best in the IGD⁺ indicator on the majority of instances (statistically significant difference for $p < 0.01$, see fig. 11), which can be due to the crowding distance estimation to maintain diversity which is beneficial

	DNSGAI	NSGAI	NSGAI
NO_X14_Y14_PM_K3_BF	0.17825 (0.051749)*	0.072188 (0.032839)	0.24099 (0.11487)*

TABLE I

OBTAINED MEDIAN AND IQR VALUES FOR THE IGD^+ INDICATOR ON THE DIFFERENT ALGORITHMS. BEST PERFORMANCE IS SHOWN IN BOLD. AN ASTERISK (*) INDICATES STATISTICAL SIGNIFICANCE COMPARED TO THE RESPECTIVE BEST ALGORITHM.

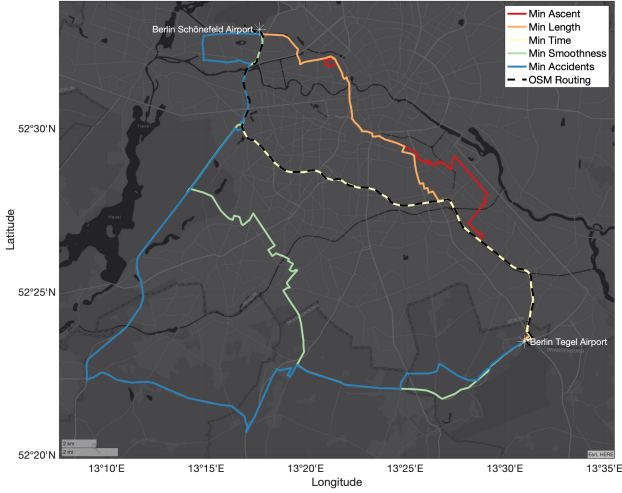


Fig. 6. Map of Berlin showing the best path in terms of each objective. **—** Min Ascent, **—** Min Length, **—** Min Time, **—** Min Smoothness, **—** Min delay, the dashed black line represents the route from the original OpenStreetMap Routing Service

to irregular Pareto-fronts [40].

We provide all obtained graphs in the supplementary material for further analysis.

D. Real-World Data

In the following, we aim to transfer the problem from the proposed benchmark to a real-world application. We use the data on the map of Berlin and compute a set of paths between the two airports *Berlin-Tegel* and *Berlin-Schönefeld*. For this purpose, we use OpenStreetMap data which we imported and converted to an undirected graph via the *osmnx* library [45]. We simplify the network by removing nodes which do not represent an intersection. The resulting graph has 63731 vertices and 84912 edges. For merged edges, we took the maximum values of the merged partners and aggregated the distances. Due to this, our computed path is an approximation but can be used to analyse the algorithm’s performance on real-world data. Figure 6 shows the layout of the map and depicts the start and endpoint.

The OpenStreetMap provides the GPS-coordinates for a grid representation which can be easily used to measure the

	DNSGAI	NSGAI	NSGAI
REALMAP	0.17849 (0.082822)*	0.11123 (0.056836)	0.11023 (0.049451)

TABLE II

OBTAINED MEDIAN AND IQR VALUES FOR THE IGD^+ INDICATOR ON THE DIFFERENT ALGORITHMS. BEST PERFORMANCE IS SHOWN IN BOLD. AN ASTERISK (*) INDICATES STATISTICAL SIGNIFICANCE COMPARED TO THE RESPECTIVE BEST ALGORITHM.

path length for the first objective. As for the second objective concerning the delay (number of accidents), we used the publicly available accident statistic data² and mapped them to the imported network. Since the coordinates of the accidents are mostly different from the available nodes in the network, we defined an R-Tree-Index on the network and performed a nearest node search for each accident. In this way, we aligned each accident to a node in the network. The third objective was measured using the Google Maps Elevation API³. The elevation is obtained in meters over the sea level and written to the node’s properties. For the smoothness, we simplified the network to straight connections between nodes. Therefore, it is obtained in the same way as in the proposed benchmark. From the OpenStreetMap network, we could also obtain the information about speed limits per street segment. We calculated the time needed per segment as the ratio of distance and speed. Summing up the values of each segment results in the total traveling time (Objective 5). For the experiments, we take the same parameter settings as above with only one-point cross-over.

Since this is a real-world problem, we do not know the true Pareto-front. In order to approximate the performance of the algorithms, we combined all results from all three algorithms and all 31 runs and calculated the non-dominated solution set. We obtained 1422 non-dominated solutions. Figure 6 shows a subset of the obtained non-dominated solutions and the route obtained from the OpenStreetMap routing service. For clarity, we do not depict the whole set, as the number of non-dominated solutions usually increases with an increasing amount of objectives. The figure shows five non-dominated routes from one airport to the other, representing the best solution per objective. It is visible that the routes have differences. Furthermore, the route of the least accidents is mostly going over highways, indicating that the algorithms could explore the search space. Interestingly, our obtained route with the least time is the same as the obtained one from the OSM routing service. With the obtained reference from all runs, we were able to calculate the IGD^+ indicator for the three algorithms. ?? shows the obtained results in terms of statistical significance, fig. 7 shows the respective values. Figure 8 shows the parallel plot of the best solutions per objective.

E. Benchmark vs Real-World

We performed the three algorithms on several benchmark instances as well as on simplified real-world data. We obtained a reference front from the real-world example by combining all results and determining the non-dominated solution set. To compare our benchmark framework to real-world data and to evaluate how much it represents actual environments, we look at some plots showing the true Pareto-fronts and obtained reference fronts. Figure 9 shows two plots of the pairwise non-dominated solution set between the objectives *Ascent* and *Accidents*. The shapes have similar characteristics, but the front from the benchmark instance also has at least

²https://unfallatlas.statistikportal.de/_opendata2019.html

³<https://developers.google.com/maps/documentation/elevation/start>

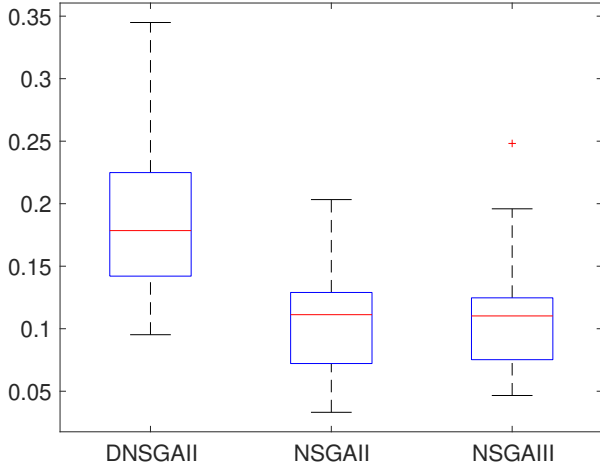


Fig. 7. Obtained IGD^+ values on Real-world problem

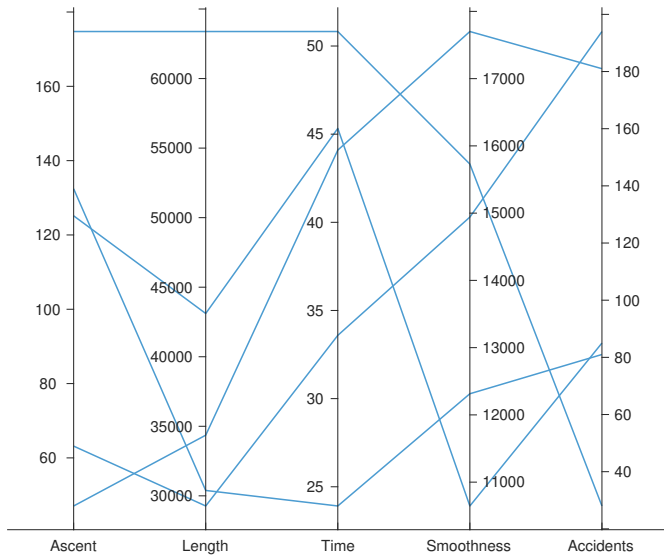


Fig. 8. Parallel coordinates plot of the best paths per objective.

one specific visible knee point. When comparing *Length* and *Accidents* is it visible, that the real-world front has clusters where the benchmark one is more distributed. The comparison of these two experiments also has several drawbacks as the benchmark instance is derived from a grid; hence from an evenly distributed environment. The real-world experiment is solely based on actual data which is mostly not evenly distributed, depending on the location which is represented. The cartesian grid-based benchmark may represent block-like environments better. To bring this more into perspective, in the analysed benchmarks, we computed a corner-to-corner path. For other start and endpoints, the fronts can look completely different.

We performed another, preferably visual, comparison with an industry used route planning software provided by the *osmr-project*⁴. The official OpenStreetMap routing service uses the project. As visible in fig. 6 the dashed line and the line of the best path in terms of time overlap entirely. This

⁴<http://project-osrm.org/>

indicates that our algorithm found the best route in terms of time, assuming that the service calculates an optimal single-objective route.

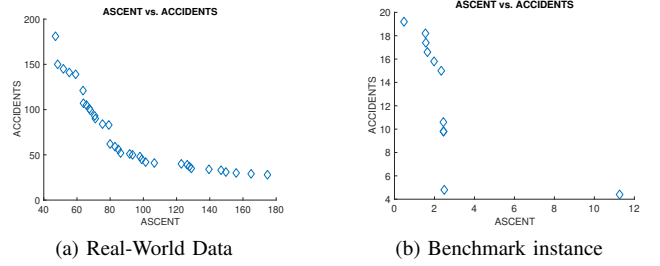


Fig. 9. Plots of the pairwise front between the Ascent-objective and the Accidents-objective on the real-world data and the instance ASLETISMAC_NO_X14_Y14_PM_K3_BF

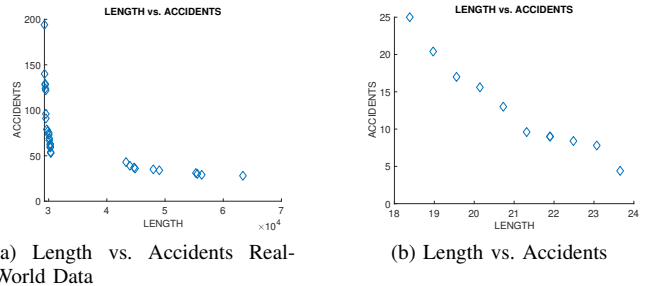


Fig. 10. Plots of the pairwise front between the Length-objective and the Accidents-objective on the real-map instance and the benchmarking instance: ASLETISMAC_NO_X14_Y14_PM_K3_BF

VI. CONCLUSION

In this paper, we present a variable many-objective pathfinding benchmark problem framework together with a model which can be easily transferred to a real-world related navigation problem on actual map data. The benchmark is scalable and can be used to analyse many-objective optimisation techniques for route planning and navigation. Different obstacle types, as well as elevation functions, neighbourhoods and backtracking properties, can be adjusted according to the needed complexity. We proposed five objective functions for the benchmark related to real-world goals when planning a route. Furthermore, we obtained the true Pareto-fronts for several benchmark instances which we also provide in the supplementary material.

Additionally, we applied three evolutionary algorithms to minimise five objectives and compared the results with the obtained true Pareto-front of several benchmark problem instances. Also, we transferred the benchmark's characteristics to real-world data by adding further information to an obtained OpenStreetMap data graph. We also applied the algorithms with the same parameters and could obtain promising results. In the future, we will work on advanced algorithms and operators to work on our benchmark. Besides, we aim to analyse more extensive and more complex instances of the problem, specifically the instances with enabled backtracking. As this will increase the search space by several magnitudes,

we also aim to investigate more sophisticated methods to obtain the true Pareto-fronts of more complex instances. Additionally, we want to increase the number of objectives and will also investigate dynamically changing objectives, e.g. traffic data, which is often taken into account when using current route planning systems. Furthermore, we will work on robustness measurements when the environment contains uncertainties. We also plan to analyse the real-world data further to provide more realistic benchmark instances. Eventually, we want to encourage the community to analyse the instances even further and apply their algorithms on the problem.

APPENDIX A REFERENCES

- [1] P. Toth and D. Vigo, *Vehicle routing: problems, methods, and applications*. SIAM, 2014. [Online]. Available: <https://epubs.siam.org/doi/pdf/10.1137/1.9781611973594.fm>
- [2] F. Ahmed and K. Deb, "Multi-objective optimal path planning using elitist non-dominated sorting genetic algorithms," *Soft Computing*, vol. 17, no. 7, pp. 1283–1299, 7 2013. [Online]. Available: <http://dx.doi.org/10.1007/s00500-012-0964-8><http://link.springer.com/10.1007/s00500-012-0964-8><http://www.iitk.ac.in/kangal/pub.htm>
- [3] O. Castillo, L. Trujillo, and P. Melin, "Multiple objective genetic algorithms for path-planning optimization in autonomous mobile robots," *Soft Computing*, vol. 11, no. 3, pp. 269–279, 2 2007. [Online]. Available: <http://link.springer.com/10.1007/s00500-006-0068-4>
- [4] M. Alajlan, A. Koubaa, I. Chaari, H. Bennaceur, and A. Ammar, "Global path planning for mobile robots in large-scale grid environments using genetic algorithms," in *2013 International Conference on Individual and Collective Behaviors in Robotics (ICBR)*, no. 1. IEEE, 2013, pp. 1–8. [Online]. Available: <http://ieeexplore.ieee.org/document/6729271/>
- [5] F. Ahmed and K. Deb, "Multi-objective path planning using spline representation," *2011 IEEE International Conference on Robotics and Biomimetics, ROBIO 2011*, no. 2011010, pp. 1047–1052, 2011.
- [6] L. Changan, Y. Xiaohu, L. Chunyang, and L. I. Guodong, "Dynamic Path Planning for Mobile Robot Based on Improved Genetic Algorithm," *Chinese Journal of Electronics*, vol. 19, no. 2, 2010.
- [7] Z. Qiongbing and D. Lixin, "A new crossover mechanism for genetic algorithms with variable-length chromosomes for path optimization problems," *Expert Systems with Applications*, vol. 60, pp. 183–189, 10 2016. [Online]. Available: <http://dx.doi.org/10.1016/j.eswa.2016.04.005><https://linkinghub.elsevier.com/retrieve/pii/S0957417416301634>
- [8] B. Tozer, T. Mazzuchi, and S. Sarkani, "Many-objective stochastic path finding using reinforcement learning," *Expert Systems with Applications*, vol. 72, pp. 371–382, 4 2017. [Online]. Available: <http://dx.doi.org/10.1016/j.eswa.2016.10.045><https://linkinghub.elsevier.com/retrieve/pii/S0957417416305863>
- [9] F.-J. J. Pulido, L. Mandow, and J.-L. L. Pérez-De-La-Cruz, "Dimensionality reduction in multiobjective shortest path search," *Computers & Operations Research*, vol. 64, pp. 60–70, 7 2015. [Online]. Available: <http://dx.doi.org/10.1016/j.cor.2015.05.007><https://linkinghub.elsevier.com/retrieve/pii/S0305054815001240>
- [10] M. Rajabi-Bahaabadi, A. Shariat-Mohaymany, M. Babaei, and C. W. Ahn, "Multi-objective path finding in stochastic time-dependent road networks using non-dominated sorting genetic algorithm," *Expert Systems with Applications*, vol. 42, no. 12, pp. 5056–5064, 7 2015. [Online]. Available: <http://dx.doi.org/10.1016/j.eswa.2015.02.046><https://linkinghub.elsevier.com/retrieve/pii/S0957417415001530>
- [11] J. Weise, S. Benkhardt, and S. Mostaghim, "A Survey on Graph-based Systems in Manufacturing Processes," in *2018 IEEE Symposium Series on Computational Intelligence (SSCI)*. IEEE, 11 2018, pp. 112–119. [Online]. Available: <https://ieeexplore.ieee.org/document/8628683/>
- [12] K. Yakovlev, E. Baskin, and I. Hramoin, "Grid-Based Angle-Constrained Path Planning," in *Lecture Notes in Computer Science (including subseries Lecture Notes in Artificial Intelligence and Lecture Notes in Bioinformatics)*, 2015, vol. 9324, pp. 208–221. [Online]. Available: http://dx.doi.org/10.1007/978-3-319-24489-1_16
- [13] A. Elshamli, H. A. Abdullah, and S. Areibi, "Genetic algorithm for dynamic path planning," in *Canadian Conference on Electrical and Computer Engineering 2004 (IEEE Cat. No.04CH37513)*, vol. 2. IEEE, 2004, pp. 677–680. [Online]. Available: <http://ieeexplore.ieee.org/document/1345203/>
- [14] J. Hu, Q. Zhu, H. Jun, and Z. Qingbao, "Multi-objective Mobile Robot Path Planning Based on Improved Genetic Algorithm," in *2010 International Conference on Intelligent Computation Technology and Automation*, vol. 2. IEEE, 2010, pp. 752–756. [Online]. Available: <http://ieeexplore.ieee.org/document/5522628/>
- [15] S. Mittal, K. Deb, Shashi Mittal, and Kalyanmoy Deb, "Three-dimensional offline path planning for UAVs using multiobjective evolutionary algorithms," in *2007 IEEE Congress on Evolutionary Computation*. IEEE, 2007, pp. 3195–3202. [Online]. Available: <http://ieeexplore.ieee.org/document/4424880/>
- [16] M. Davoodi, F. Panahi, A. Mohades, and S. N. Hashemi, "Multi-objective path planning in discrete space," *Applied Soft Computing*, vol. 13, no. 1, pp. 709–720, 1 2013. [Online]. Available: <http://dx.doi.org/10.1016/j.asoc.2012.07.023><https://linkinghub.elsevier.com/retrieve/pii/S1568494612003407>
- [17] E. Besada-Portas, L. de la Torre, A. Moreno, and J. L. Risco-Martín, "On the performance comparison of multi-objective evolutionary UAV path planners," *Information Sciences*, vol. 238, pp. 111–125, 7 2013. [Online]. Available: <http://dx.doi.org/10.1016/j.ins.2013.02.022><https://linkinghub.elsevier.com/retrieve/pii/S0020025513001394>
- [18] H. Qu, K. King, and T. Alexander, "An improved genetic algorithm with co-evolutionary strategy for global path planning of multiple mobile robots," *Neurocomputing*, vol. 120, pp. 509–517, 11 2013. [Online]. Available: <http://dx.doi.org/10.1016/j.neucom.2013.04.020><https://linkinghub.elsevier.com/retrieve/pii/S0925231213005195>
- [19] N. R. Sturtevant, "Benchmarks for Grid-Based Pathfinding," *IEEE Transactions on Computational Intelligence and AI in Games*, vol. 4, no. 2, pp. 144–148, 2012. [Online]. Available: <http://ieeexplore.ieee.org/document/6194296/>
- [20] S. Koceski, S. Panov, N. Koceska, P. B. Zobel, and F. Durante, "A Novel Quad Harmony Search Algorithm for Grid-Based Path Finding," *International Journal of Advanced Robotic Systems*, vol. 11, no. 9, p. 144, 9 2014. [Online]. Available: <http://journals.sagepub.com/doi/10.5772/58875>
- [21] B. Anguelov, "Video Game Pathfinding and Improvements to Discrete Search on Grid-based Maps," Ph.D. dissertation, 2011. [Online]. Available: <http://cirg.cs.up.ac.za/>
- [22] A. R., "Path Finding Solutions For Grid Based Graph," *Advanced Computing: An International Journal*, vol. 4, no. 2, pp. 51–60, 3 2013. [Online]. Available: <http://www.aircse.org/journal/acij/papers/4213acij05.pdf>
- [23] J. Xiao and Z. Michalewicz, "An Evolutionary Computation Approach to Robot Planning and Navigation," *Soft Computing in Mechatronics*, vol. 32, pp. 117–141, 1999. [Online]. Available: https://books.google.de/books?hl=de&lr=&id=v8n_Kdp5FEC&oi=fnd&pg=PA117&dq=related:af40VagNBO4J:scholar.google.com/&ots=6HFJ_-Bx1j&sig=fpnpbGdJF3Oq-ScO8Ll6LbIKvh0
- [24] P. Yap, "Grid-Based Path-Finding," in *Lecture Notes in Computer Science (including subseries Lecture Notes in Artificial Intelligence and Lecture Notes in Bioinformatics)*, 2002, vol. 2338, pp. 44–55. [Online]. Available: http://link.springer.com/10.1007/3-540-47922-8_4
- [25] G. Belov, L. Cohen, M. G. de la Banda, D. Harabor, S. Koenig, and X. Wei, "Position Paper: From Multi-Agent Pathfinding to Pipe Routing," no. May, 5 2019. [Online]. Available: <http://arxiv.org/abs/1905.08412>
- [26] J. Weise, S. Benkhardt, and S. Mostaghim, "Graph-based multi-objective generation of customised wiring harnesses," in *Proceedings of the Genetic and Evolutionary Computation Conference Companion*. New York, NY, USA: ACM, 7 2019, pp. 407–408. [Online]. Available: <http://dl.acm.org/citation.cfm?doid=3319619.3321908><https://dl.acm.org/doi/10.1145/3319619.3321908>
- [27] B. K. Oleiwi, H. Roth, and B. I. Kazem, "Modified Genetic Algorithm based on A* Algorithm of Multi Objective Optimization for Path Planning," *Journal of Automation and Control Engineering*, vol. 2, no. 4, pp. 357–362, 2014.
- [28] L. Mandow and J. L. P. De La Cruz, "Multiobjective A* search with consistent heuristics," *Journal of the ACM*, vol. 57, no. 5, pp. 1–25, 6 2010. [Online]. Available: <http://portal.acm.org/citation.cfm?doid=1754399.1754400>
- [29] P. E. Hart, N. J. Nilsson, and B. Raphael, "A Formal Basis for the Heuristic Determination of Minimum Cost Paths," *IEEE Transactions on Systems Science and Cybernetics*, vol. 4, no. 2, pp. 100–107, 1968.

- [30] J. E. Fieldsend, T. Chugh, R. Allmendinger, and K. Miettinen, "A feature rich distance-based many-objective visualisable test problem generator," in *Proceedings of the Genetic and Evolutionary Computation Conference*. New York, NY, USA: ACM, 7 2019, pp. 541–549. [Online]. Available: <http://dl.acm.org/doi/10.1145/3321707.3321727><https://dl.acm.org/doi/10.1145/3321707.3321727>
- [31] K. Deb, L. Thiele, M. Laumanns, and E. Zitzler, "Scalable Test Problems for Evolutionary Multiobjective Optimization," in *Evolutionary Multiobjective Optimization*. London: Springer-Verlag, pp. 105–145. [Online]. Available: http://link.springer.com/10.1007/1-84628-137-7_6
- [32] A. Raith and M. Ehrgott, "A comparison of solution strategies for biobjective shortest path problems," *Computers & Operations Research*, vol. 36, no. 4, pp. 1299–1331, 4 2009. [Online]. Available: <https://linkinghub.elsevier.com/retrieve/pii/S0305054808000233>
- [33] R. Stern, N. R. Sturtevant, A. Felner, S. Koenig, H. Ma, T. T. Walker, J. Li, D. Atzmon, L. Cohen, T. K. S. Kumar, E. Boyarski, R. Bartak, R. Bart, R. Bartak, T. K. Satish Kumar, E. Boyarski, and R. Barták, "Multi-Agent Pathfinding: Definitions, Variants, and Benchmarks," no. SoCS, pp. 151–158, 6 2019. [Online]. Available: [www.aaai.orghttp://arxiv.org/abs/1906.08291](http://arxiv.org/abs/1906.08291)
- [34] C. Lamini, S. Benhlima, and A. Elbekri, "Genetic algorithm based approach for autonomous mobile robot path planning," *Procedia Computer Science*, vol. 127, pp. 180–189, 2018. [Online]. Available: <https://doi.org/10.1016/j.procs.2018.01.113>
- [35] A. Tuncer and M. Yildirim, "Dynamic path planning of mobile robots with improved genetic algorithm," *Computers and Electrical Engineering*, vol. 38, no. 6, pp. 1564–1572, 11 2012. [Online]. Available: <http://dx.doi.org/10.1016/j.compeleceng.2012.06.016>
- [36] Q. Li, W. Zhang, Y. Yin, Z. Wang, G. Liu, and Z. Wang Guangjun Liu, "An Improved Genetic Algorithm of Optimum Path Planning for Mobile Robots," in *Sixth International Conference on Intelligent Systems Design and Applications*, vol. 2. IEEE, 2006, pp. 637–642. [Online]. Available: <http://ieeexplore.ieee.org/document/4021738/>
- [37] L. Beke, M. Weiszner, and J. Chen, "A Comparison of Genetic Representations for Multi-objective Shortest Path Problems on Multigraphs." Springer International Publishing, 2020, vol. 8, no. 2010, pp. 35–50.
- [38] K. Deb, A. Pratap, S. Agarwal, and T. Meyarivan, "A fast and elitist multiobjective genetic algorithm: NSGA-II," *IEEE Transactions on Evolutionary Computation*, vol. 6, no. 2, pp. 182–197, 2002. [Online]. Available: <http://ieeexplore.ieee.org/document/996017/>
- [39] K. Deb and H. Jain, "An Evolutionary Many-Objective Optimization Algorithm Using Reference-Point-Based Nondominated Sorting Approach, Part I: Solving Problems With Box Constraints," *IEEE Transactions on Evolutionary Computation*, vol. 18, no. 4, pp. 577–601, 2014. [Online]. Available: <http://ieeexplore.ieee.org/document/6600851/>
- [40] X. Cai, H. Sun, and Z. Fan, "A diversity indicator based on reference vectors for many-objective optimization," *Information Sciences*, vol. 430–431, pp. 467–486, 3 2018. [Online]. Available: <https://linkinghub.elsevier.com/retrieve/pii/S0020025517311155>
- [41] D. Michail, J. Kinable, B. Naveh, and J. V. Sichi, "JGraphT – A Java library for graph data structures and algorithms," 4 2019. [Online]. Available: <http://arxiv.org/abs/1904.08355>
- [42] A. J. Nebro, J. J. Durillo, and M. Vergne, "Redesigning the jMetal Multi-Objective Optimization Framework," in *Proceedings of the Companion Publication of the 2015 on Genetic and Evolutionary Computation Conference - GECCO Companion '15*. New York, New York, USA: ACM Press, 7 2015, pp. 1093–1100. [Online]. Available: <http://dl.acm.org/citation.cfm?doid=2739482.2768462>
- [43] H. Ishibuchi, H. Masuda, and Y. Nojima, "A Study on Performance Evaluation Ability of a Modified Inverted Generational Distance Indicator," in *Proceedings of the 2015 on Genetic and Evolutionary Computation Conference - GECCO '15*. New York, New York, USA: ACM Press, 7 2015, pp. 695–702. [Online]. Available: <http://dl.acm.org/citation.cfm?doid=2739480.2754792>
- [44] H. Ishibuchi, H. Masuda, Y. Tanigaki, and Y. Nojima, "Difficulties in specifying reference points to calculate the inverted generational distance for many-objective optimization problems," in *2014 IEEE Symposium on Computational Intelligence in Multi-Criteria Decision-Making (MCDM)*. IEEE, 2014, pp. 170–177. [Online]. Available: <http://ieeexplore.ieee.org/lpdocs/epic03/wrapper.htm?arnumber=7007204>
- [45] G. Boeing, "OSMnx: New methods for acquiring, constructing, analyzing, and visualizing complex street networks," *Computers, Environment and Urban Systems*, vol. 65, pp. 126–139, 9 2017. [Online]. Available: <http://dx.doi.org/10.1016/j.compenurbsys.2017.05.004><https://linkinghub.elsevier.com/retrieve/pii/S0198971516303970>



Jens Weise received his B.Sc. degree in computer systems in engineering and his M.Sc. in medical systems engineering at the Otto von Guericke University Magdeburg, in 2013 and 2017 respectively. His current research includes many-objective pathfinding and route planning using evolutionary multi-objective optimisation methods. He also researches on methods of self-organisation in the field of factory planning.



Sanaz Mostaghim is a full professor of computer science at the Otto von Guericke University Magdeburg, Germany. She holds a PhD degree in electrical engineering and computer science from the University of Paderborn, Germany. She worked as a post-doctoral fellow at ETH Zurich in Switzerland and as a lecturer at Karlsruhe Institute of technology (KIT), Germany. Her research interests are in the area of evolutionary multi-objective optimization, swarm intelligence, and their applications in robotics, science and industry. She serves as an associate editor for the *IEEE Transactions on Evolutionary Computation*, *IEEE Transactions on Cybernetics*, *IEEE Transactions on System, Man and Cybernetics: Systems* and *IEEE Transactions on Emerging Topics in Computational Intelligence*.

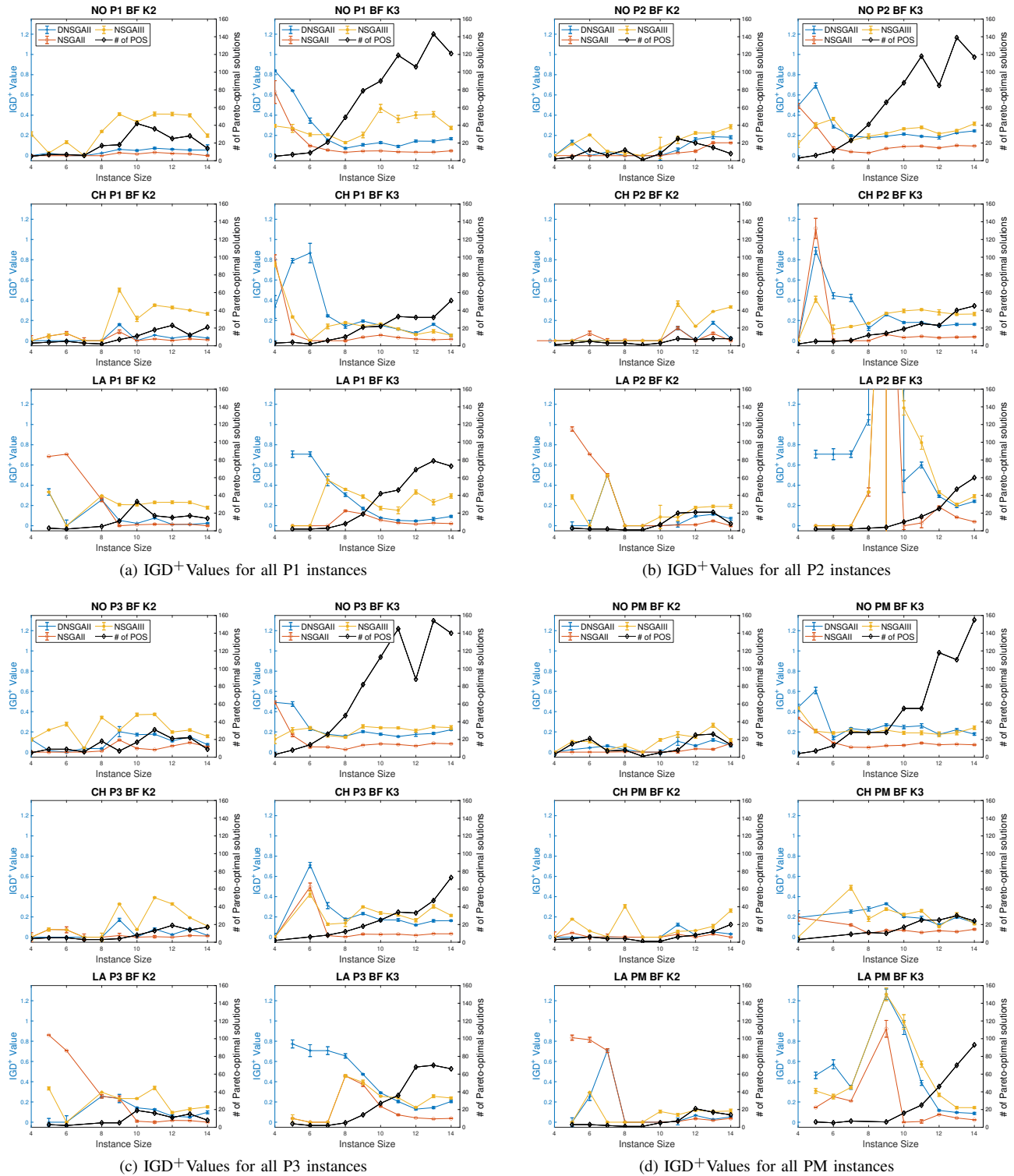


Fig. 11. The obtained IGD⁺ values with respect to the different type, ordered by instance size.